Annales Societatis Geologorum Poloniae (2012), vol. 82: 255–262.

PHENOMENA AT INTERFACE OF SALINE AQUIFER AND CLAYSTONE CAPROCK UNDER CONDITIONS OF CO_2 STORAGE

Krzysztof LABUS

Silesian University of Technology, Institute for Applied Geology, 2 Akademicka St., 44-100 Gliwice, Poland,
e-mail: krzysztof.labus@polsl.pl

Labus, K., 2012. Phenomena at interface of saline aquifer and claystone caprock under conditions of CO_2 storage. *Annales Societatis Geologorum Poloniae*, 82: 255–262.

Abstract. When modelling the impact of the hydrogeochemical processes of CO_2 sequestration on the contact zone of a saline sandstone aquifer and a claystone caprock in the Upper Silesian Coal Basin, small decreases in porosity were noted, visible mainly in the aquifer rocks. They were due to the degradation of kaolinite, albite and muscovite, and the recrystallization of K-feldspar and quartz. The porosity of the caprock remained almost unchanged, which was to the advantage of the integrity of the repository. In major parts of the aquifer and caprock zone, the mineral trapping of CO_2 has beneficial effects, but at the interface of the aquifer and the insulating layer, in the basal part of the caprock, a release of carbon dioxide may occur temporarily, associated with the dissolution of calcite.

Key words: aquifer CO_2 sequestration, gas–rock–water interactions, caprock reactivity, geochemical modelling, Upper Silesian Coal Basin.

Manuscript received 5 September 2012, accepted 20 December 2012

INTRODUCTION

Long-term, geological storage of CO_2 requires reliability and integrity of the caprocks, isolating the repository, to prevent any escape of the gas. From this point of view, laboratory experiments and modelling studies, which yield insight into the specificity of gas–water–rock interactions within the aquifer–caprock contact zones, are of special importance.

The textural evolution of caprocks and changes to their integrity still merit further study. However previous work (Johnson *et al.*, 2004; Gaus *et al.*, 2005; Xu *et al.*, 2005; Credoz *et al.*, 2009; Bildstein *et al.*, 2010) permits deeper understanding of these issues. One of the first batch experiments, performed by Kaszuba *et al.* (2005), dealt with aquifer and aquitard as one system, in which the gas–water–rock interactions in the aquifer influenced the pore-water composition at the contact with the caprock. Their observations proved the possible reactivity of caprock shales. The CO_2 injection caused an initial pH decrease. The reaction later was increased, which was interpreted as a consequence of the trapping of dissolved CO_2 in the mineral phases.

The Sleipner injection site was studied by Gaus et al. (2005), who simulated the impact of CO_2 on a clayey caprock. According to their research, only a few meters of the caprock will be altered in thousands of years, owing to the low, effective diffusion of CO_2. This effect is enhanced by the precipitation of secondary chalcedony, kaolinite and calcite, which are products of CO_2-caprock interaction.

Bildstein *et al.* (2010) used various, reactive transport modelling codes to conduct numerical simulations of caprock behavior after the CO_2 injection. Significant porosity changes in the carbonate-rich caprock, limited to the aquifer-caprock interface zone, were observed. It was also found that the opening of fractures, mainly filled with calcite, creates possible migration paths of CO_2 into the caprock.

A modern set of techniques was employed by Navarre-Sitchler *et al.* (2011) to examine the evolution of pore spaces,, forced by CO_2 injection. Their methods enable obtaining quantitative information, and include 3-D pore reconstructions and small-angle neutron scattering (SANS).

Also the effects of co-injection of CO_2 with H_2S and SO_2 impurities, typical for the flue gas from conventional power generation, were studied by Xu *et al.* (2007) and Xiao *et al.* (2009). Their results prove the different behavior of reservoir rocks, connected to strong acidic environments, but the response of the caprock still needs additional research.

An extensive review of the published experimental works, modelling and field observations of CO_2–brine–caprock interactions was presented by Liu *et al.* (2012), who reported that geochemical modelling, based on thermodynamics and kinetics, must be employed to extrapolate short-term laboratory experiment results to the assessment of the long-term effects of storage. With this aim in mind,

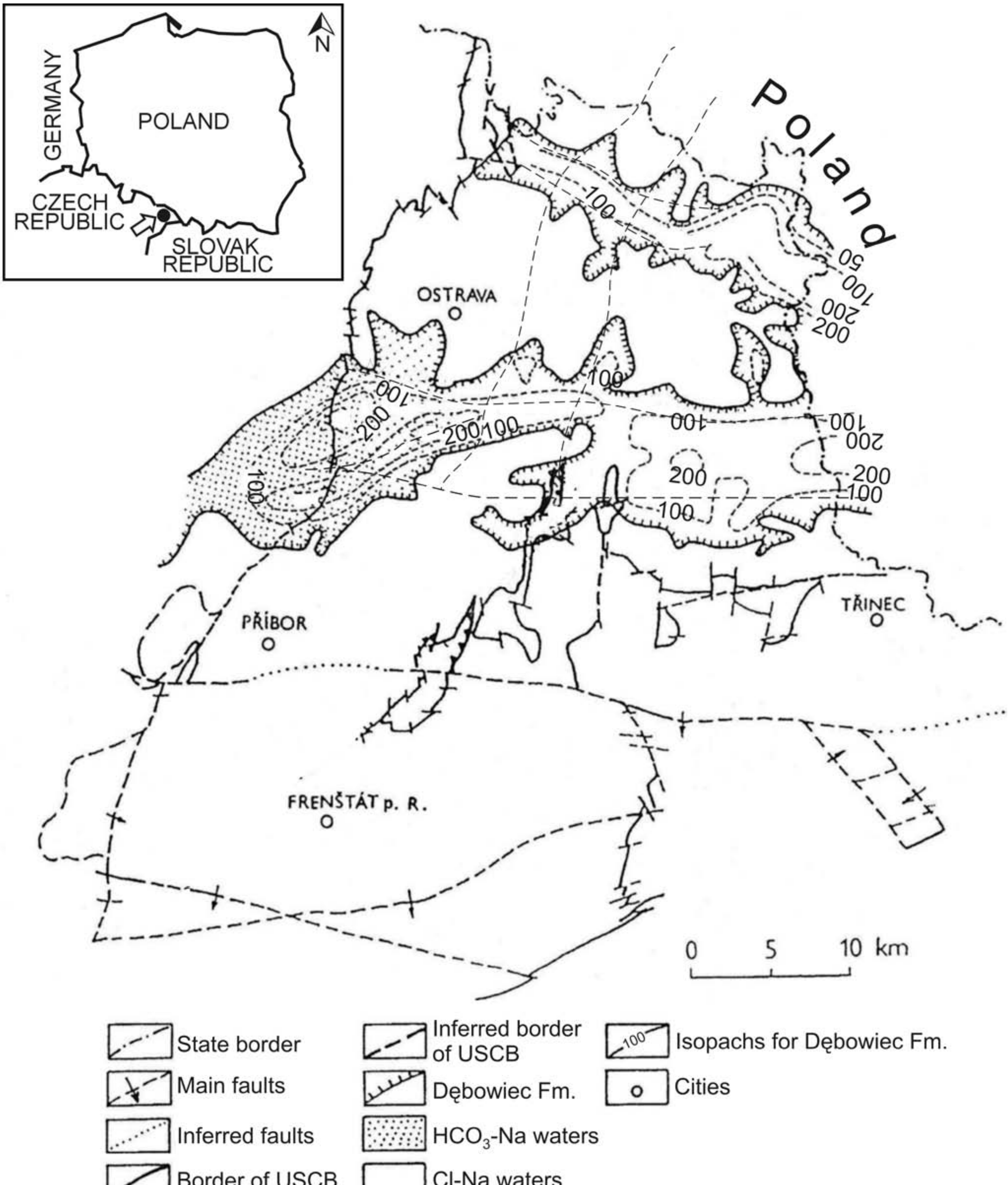

Fig. 1. Dębowiec Formation in western part of Upper Silesian Coal Basin (USCB) (after Labus, 2005; modified)

the modelling of batch experiments that yielded mineralogical analysis, as well as solution chemistry, will be required.

Evaluation of mineral trapping mechanisms and assessment of storage capacity of the aquifer and caprocks of the Upper Silesian Coal Basin (USCB), based on hydrochemical modelling and experimental tests of rock–water–gas interactions, was done also by Labus and Bujok (2011). Two stages of modelling enabled prediction of the immediate changes in the aquifer and insulating rocks, impacted by the onset of CO_2 injection, and the assessment of the long-term effects of sequestration. In the sandstone aquifers analyzed, the minerals, able to trap CO_2, are dawsonite and

Table 1

Composition of pore waters in caprock and aquifer, used in computer simulation

Parameter	Unit	Caprock	Aquifer
Porosity		0.05	0.13
fCO_2	MPa	4.7	4.7
T	°C	30	30
Na^+	mg/kg	19890	12270
K+	mg/kg	22.48	5.9
Ca^{2+}	mg/kg	3078	964
Mg^{2+}	mg/kg	128.1	105.2
HCO^{3-}	mg/kg	110	38.1
Cl^-	mg/kg	24860	20910
SO_4^{2-}	mg/kg	4710	5.88
$SiO_{2(aq)}$	mg/kg	5.44	8.86
Al^{3+}	mg/kg	0.002	0.004
Fe^{2+}	mg/kg	41.78	0.7
pH	-	6.81	7.37
TDS	mg/kg	52848	34311

dolomite, while siderite and calcite degrade. The phases, capable of mineral trapping of CO_2 in the cap rocks, are dawsonite, dolomite, and siderite. Mineral trapping capacity for the sandstone aquifers is relatively low at 1.2 to 1.9 kg CO_2/m^3, with the exception of the Upper Silesian Sandstone Series, at over 6.6 kg CO_2/m^3. The solubility trapping capacity does not exceed 4.07 kg CO_2/m^3.

The purpose of this study was to determine the behavior of the aquifer rock of the Dębowiec Formation (Miocene) and the insulating rocks, in conditions of CO_2 injection into the geological media, aiming to the gas storage. Modelling was performed for the water–rock–gas system, and the results enabled the evaluation of changes in porosity and permeability of the rocks. These parameters are crucial for the injectivity and also for the safety of CO_2 geological storage. The sequestration capacity of aquifer and caprocks also was assessed, assuming that the contact zone of the insulating layer with the collector can be regarded as the zone of CO_2 trapping.

GEOLOGICAL SETTING

The area belongs to the SW part of the Upper Silesian Coal Basin (Fig. 1). The main hydrostructures of the area are the multi-aquifer formations that are Quaternary, Tertiary, and Carboniferous in age. The last two of these might be cosidered for carbon dioxide sequestration. The Tertiary sediments of the Dębowiec Conglomerates (Lower Badenian) fill deep depressions at the top of the Carboniferous strata, reaching depths of 700 m b.s.l. in the northern part and up to 1100 m b.s.l. in the southern part, respectively. These sediments are coarse sandstones, conglomerates and breccias that form an aquifer up to 268 m thick. Stagnant waters, mainly of the Cl-Na type and with an average TDS of 35g/l are typical for this structure (Labus, 2005). The insulating layer (caprock) is composed of mudstones and claystones of the Skawina Formation (Lower Badenian) and is 500–1100 m thick. Pressure, CO_2 fugacity and temperature, relevant to the depths of modelled environments, are presented in Table 1 and Fig. 2.

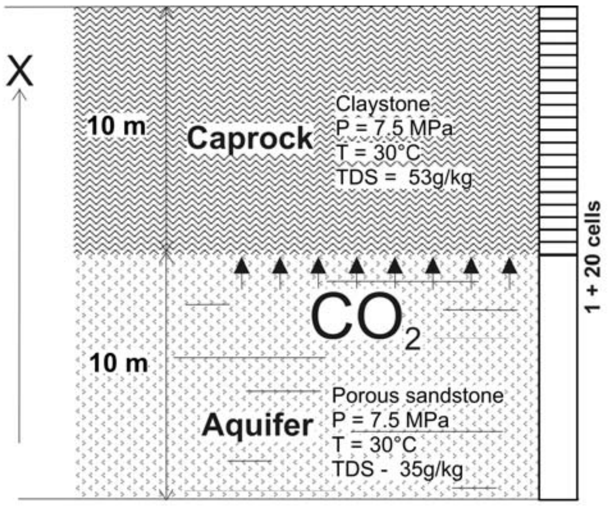

Fig. 2. One-dimensional model of aquifer-caprock contact zone in conditions of CO_2 sequestration

METHODS

In modelling the reactions and transport in conditions of CO_2 injection and storage, the Petrasim software was used, based on the TOUGHREACT simulator (Xu *et al.*, 2006). The TOUGH2 package with the ECO2N module was applied (Pruess, 2004; Spycher and Pruess, 2005). Parameters of pore waters (Table 1) for the purpose of modelling were collected during previous research projects (e.g, Labus, 2007; Labus *et al.* 2010; Labus and Bujok, 2011). The chemical composition of waters for kinetic transport models was based on the water-rock equilibria modelling, by means of the Geochemist's Workbench 8 package (Bethke, 2008). Pore waters of Cl-Na type were characterized by mineralization between 34.3 and 52.8 g/dm^3 and with a pH of 6.81 to 7.37.

The composition of mineral assemblages was determined by means of microscopy. Petrographic, planimetric analysis of thin sections was conducted using Axioscope Zeiss Microscope. SEM analyses were performed, with the use of BS 340 Tesla microscope and JSM 630 microscope with EDS Oxford (20 kV). Additional XRD analysis was performed on an HZG-4 X-ray diffractometer. For determining the porosimetric properties of the examined rocks, the Mercury Intrusion Porosimetry (Autopore 9220 Micromeritics Injection Porosimeter) was used. Specific surface areas were calculated, assuming spherical grains of different diameters for the sandstones and fine-grained rocks (Table 2).

The modelling was performed, assuming a hydrostatic regime of formation pressure. Temperature values were estimated on the basis of direct measurements and archival data (e.g. Karwasiecka, 2001). The rate parameters of water-mineral interaction kinetics (constants for modeled reac-

Table 2

Rock matrix parameters applied in modelling

Mineral	Molar volume $[cm^3/mol]$	Molecular weight [g/mol]	Specific surface areas of mineral grains $[cm^2/g]$		Mineralogical composition [%vol]	
			Caprock	Aquifer	Caprock	Aquifer
Quartz	22.69	60.08	226.56	2.27	28	75
K-feldspar	108.87	278.33	-	7.11	-	8
Muscovite	140.71	398.31	21.96	105.98	10	5
Albite	100.25	262.22	-	6.95	-	2
Kaolinite	99.52	258.16	1156.49	115.49	30	7
Illite	138.94	383.90	1085.75	1085.75	15	3
Calcite	36.93	100.09	221.41	-	12	-
Gypsum	74.69	172.17	260.29	-	5	-

Table 3

Kinetic rate parameters at 25°C

	Kinetic rate at 25°C k25 $[mol/m^2s^{-1}]$	Activation energy EA $[J\ mol^{-1}]$	Kinetic rate at 30°C k30 $[mol/m^2s^{-1}]$
Quartz	1.02·e-14	87.6	1.83·e-14
K-feldspar	3.89·e-13	38.0	5.01·e-13
Muscovite	2.82·e-14	22.0	3.26·e-14
Albite	9.12·e-13	69.8	1.45·e-12
Kaolinite	1.00·e-13	22.2	1.16·e-13
Illite	8.91·e-16	14.0	9.78·e-16
Calcite	1.55·e-06	23.5	1.81·e-06
Gypsum	1.62·e-03	-	1.63·e-03

data from Palandri and Kharaka, 2004; except for siderite (data from Steefel, 2001) and recalculated values for 30°C

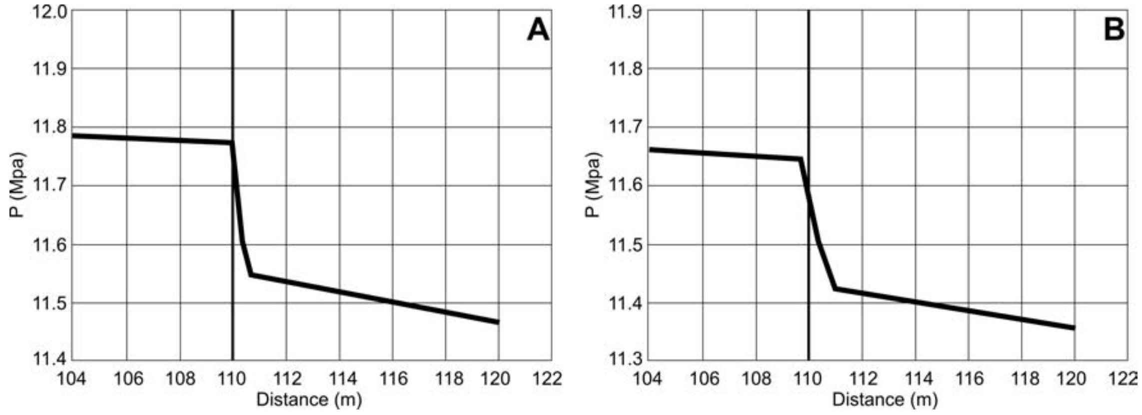

Fig. 3. Pressure in vertical distance from injection point, after: **A** – 1 year and **B** – 20000 years of storage (black line indicates interface between aquifer (left hand side) and caprock (right hand side)

tions) were taken from the literature (Palandri and Kharaka, 2004) (Table. 3).

Relative permeability of the rock matrix was calculated on the basis of the van Genuchten (1980) model for the liquid phase, and the Corey (1954) model for the gas phase. Capillary pressure was calculated on the basis of the van Genuchten (1980) model.

Modelling was performed in two stages, according to the methodology presented by Labus and Bujok (2011). The first stage was aimed at simulating the immediate changes in the aquifer and insulating rocks, affected by the beginning of CO_2 injection, lasting for 30 years (a potential lifetime of a single CCS installation); the second enabled assessment of the long-term effects of sequestration (20,000 years). The quality and progress of the reactions were monitored and their effects on formation porosity and sequestration capacity, in form of mineral, residual and the free phase of carbon dioxide, were calculated. The qualitative calibration of numerical models (including the precipitation of secondary minerals and the correction of kinetic parameters), describing the initial stage of injection, was based on the results of the experimental studies.

A model for the vertical migration of CO_2 and its impact on the aquifer–caprock contact zone was achieved by using a one-dimensional scheme (Fig. 2). According to the model, carbon dioxide is injected into the aquifer in a depth range of –750 to –850 m below the surface. From this level, it can migrate into the layer of caprock, which is 100 m thick. The model represented only the aquifer-caprock contact zone, which was simulated by means of 21 linearly arranged cells. The first cell corresponded to the upper part of the aquifer (roof of the formation), which is 10 m thick. The next 20 cells, each 0.5 m long, correspond to the caprock layer.

RESULTS AND DISCUSSION

The modelling results revealed that after the injection of CO_2, which led to a pressure increase in the aquifer to the level of 12 MPa, and to a gas-saturation of 70% of the pore space, a distinct difference (threshold) of pressures was observed between the aquifer and the caprock (Fig. 3). This difference disappeared with time and decreased from about 4.5 MPa to about 0.3 MPa, after 20 000 years (20 ka). This phenomenon was related rather to an increase of pressures in the caprock level from 7.5 MPa to 11.4 MPa, than to the pressure decline in the aquifer from 12.0 MPa to 11.7 MPa, over the analyzed time of 20 ka.

Within the aquifer, the gas saturation dropped in the time modelled from an initial value of 0.7 to about 0.65, while in

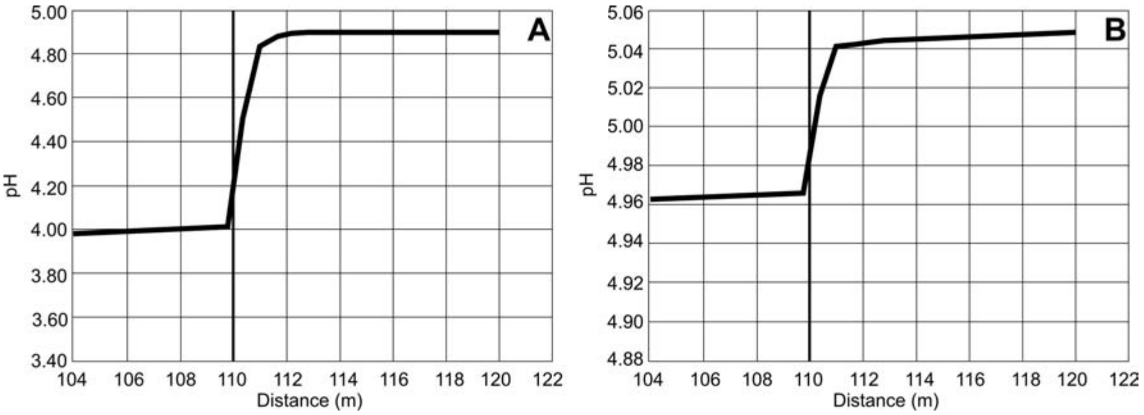

Fig. 4. Values of pH in vertical distance from injection point, after **A** – 1 year, **B** – 20,000 years of storage (explanations as in Fig. 2)

the caprock it increased from 0.05 to 0.3–0.4. Changes in pH had a tendency to rise more sharply in the aquifer than in the pore waters of overlying caprock (Fig. 4). On the basis of the microscopic observations and XRD analyses, it was determined that the rock-forming, primary minerals of the aquifer are quartz, feldspars and clay minerals. In the caprock assemblage, the dominant phases were clay minerals and quartz; calcite and gypsum were significant in terms of rock matrix reactivity.

The quantities of minerals, precipitating or dissolving, as a result of the reaction modelled, were varied (Figs 5, 7). Dissolution of calcite, about 40 mol per 1 m^3 of the formation, was observed only in the lower part of the layer of cap- rock, at the contact with the aquifer rocks. In the remaining part of the profile, the precipitation of $CaCO_3$ is noticeable, as up to 15 mol/m^3 of the formation (Fig. 5A). A considerable amount of dawsonite, in terms of CO_2 sequestration to about 140 mol/m^3, was precipitated only in the aquifer rock (Fig. 5B).

The following phenomena (Fig. 5D–G) had the greatest importance to the mineralogical and textural changes within the aquifer, during the 20 ka of storage: degradation of: kaolinite (82 mol/m^3), albite (10 mol/m^3) and muscovite (8 mol/ m^3), and the recrystallization of: K-feldspar r (60 mol/m^3), and quartz (5 mol/m^3). The transformations, involving illite (Fig. 5H) and pyrite, played a lesser role.

In the case of the caprock, the transformations in mineralogical composition and structure of the rocks over 20 ka after injection were controlled by the following processes (Figs 5C, H, E, 6): the formation of kaolinite (62 mol/m^3), and to a lesser extent, illite (1.1 mol/m^3), and the decomposition of muscovite (44 mol/m^3), and gypsum. The dissolution of quartz (0.2 mol/m^3) played a minor role (Fig. 5G).

A decrease in porosity of about 0.4% (3% relative) to the value of 12.6%, resulting from a positive balance of the volume of secondary minerals, relative to the original composition of the rocks, was visible only in the aquifer complex (Fig. 7), while in the caprock zone the porosity was constant during the time period analyzed.

After a simulated 20 ka of storage, the final pore space was assumed to be filled with CO_2 gas and pore water of known (modelled) chemical composition. The maximum values of carbon sequestration in the dissolved phase $CO_{2(aq)}$ were calculated on the basis of a mass fraction $xCO_{2(aq)}$ in pore water (Fig. 8A), for a given porosity and water saturation of the pore space. The amount of residual CO_2, contained in the pores, was calculated on the basis of gas saturation of the pore space and the known gas density (Fig. 8B). Mineral trapping capacity, the amount of CO_2 blocked in mineral phases, was assessed, taking into account the unitary volume of modelled rock (UVR), equal to 0.01 m^3 and the primary porosity (before storage), equal to n_p,. The volume of the rock matrix in 1m^3 of formation, measured in UVR units amounted to $100(1–n_p)$. Owing to the modelled reactions, certain quantities of carbonate minerals dissolved or precipitated per each UVR. On this basis, the CO_2 balance was calculated. The values of CO_2 sequestration in dissolved, gas and mineral phases after 20,000 years of storage are presented in Table 4.

The amounts of CO_2,trapped in the dissolved and residual phases, are the highest in the aquifer (7.2 kg CO_2/m^3 and 69.8 kg CO_2/m^3 respectively). This should be attributed partly to a considerable pore space volume, when compared to the cap rock, and the higher gas pressures and subsequently higher gas densities. Furthermore, greater amounts of residual gas in the aquifer were related to the elevated pressure (in comparison to the superjacent cap rock), which in turn was responsible for the higher density of the CO_2.

Mineral-trapping capacity for the Dębowiec Formation, based on the results of the modelling, was assessed at a level of 6 kg CO_2/m^3, while in the upper part of the caprock formation it was only 0.5 kg CO_2/m^3. On the other hand, for the lower part of the caprock (superjacent to the aquifer), a negative value of trapping capacity 1.2 kg CO_2/m^3 was calculated. This means that the process of dissolution of primary carbonate minerals occurs in this zone.

Table 4

Average values of CO_2 sequestered in dissolved, residual and mineral phase after 20 ka of storage

Zone	Dissolved phase	Residual phase	Mineral phases
	(kg/m^3)		
aquifer	7.19	69.8	6.0
caprock - lower part	2.55	20.49	–1.2
caprock - upper part	2.53	17.27	0.5

negative value means dissolution of primary carbonate minerals

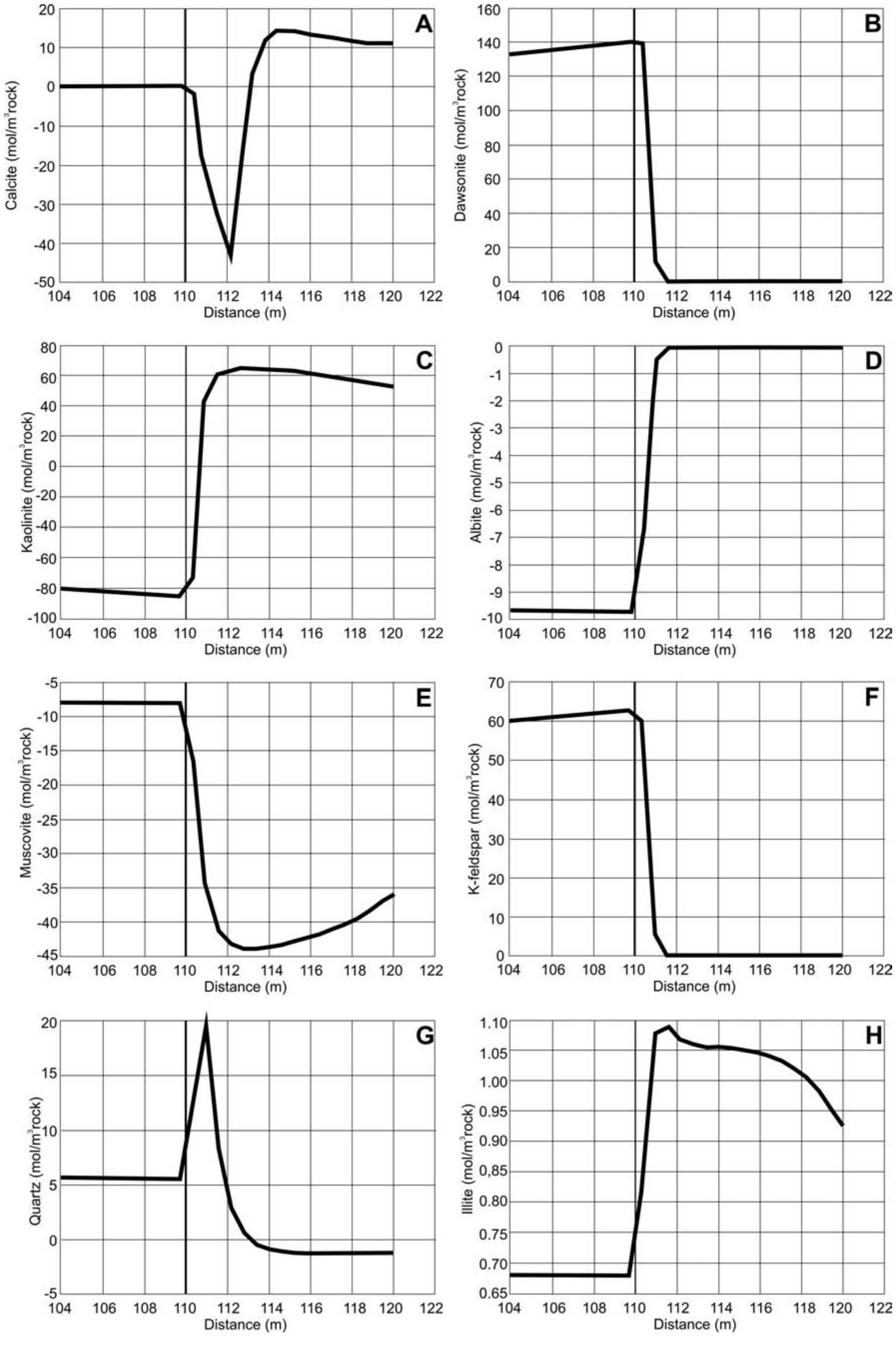

Fig. 5. Changes in amounts of minerals (mol/m^3 rock) in vertical distance from injection point after 20,000 years. **A** – calcite; **B** – dawsonite; **C** – kaolinite; **D** – albite; **E** – muscovite; **F** – K-feldspar; **G** – quartz; **H** – illite (explanations as in Fig. 2)

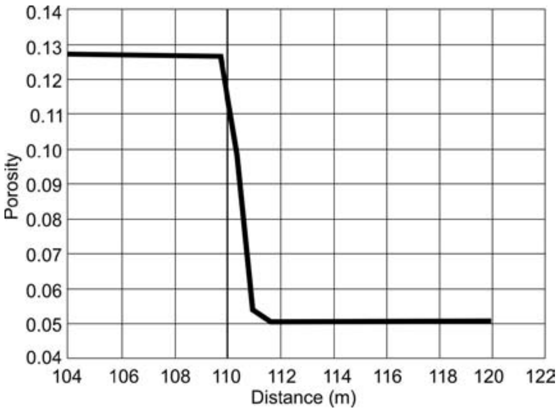

Fig. 6. Changes in amounts of gypsum (mol/m^3 rock) in vertical distance from injection point after 20,000 years (explanations as in Fig. 2)

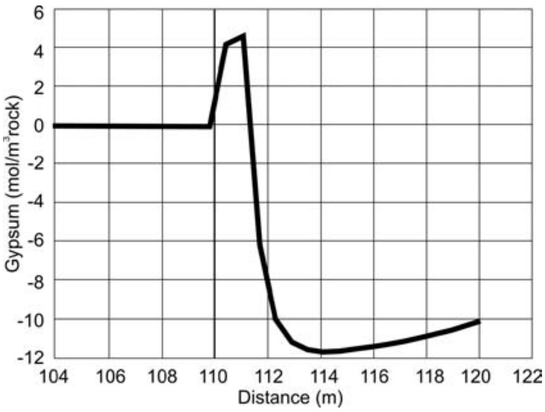

Fig. 7. Values of porosity in vertical distance from injection point after 20,000 years (explanations as in Fig. 2)

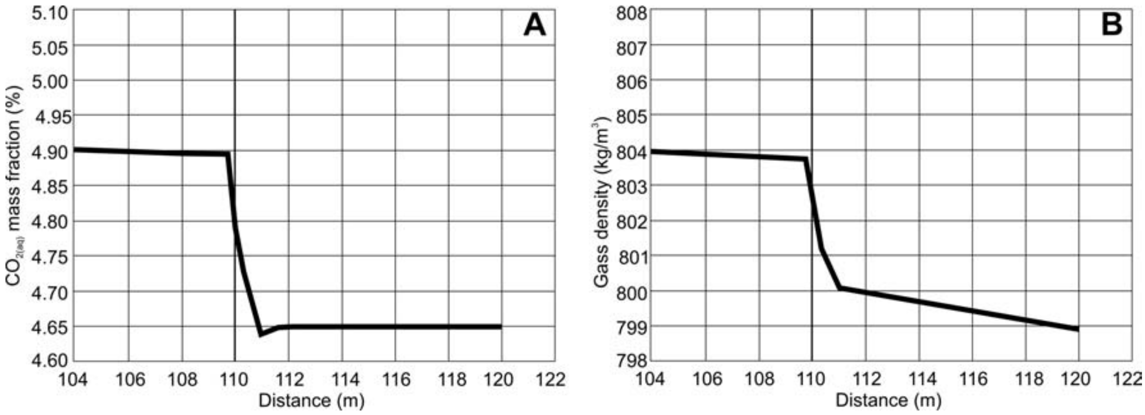

Fig. 8. Mass fraction of $CO_{2(aq)}$ – **A**, and density of CO_2 (kg/m^3) – **B** in vertical distance from injection point after 20,000 years (explanations as in the Fig. 2)

In the aquifer analyzed, the only mineral capable of trapping CO_2 is dawsonite, which is a secondary mineral in this formation. In the case of the caprock, where primary calcite is present, the dissolution of this mineral is in the lower zone, whereas at the upper zone of the cap rock, calcite precipitation efficiently blocks CO_2.

When observing the effects of mineralogical changes in the rocks analyzed, it should be noted that the processes, occurring in the contact zone between the aquifer and insulating layers, were different from those that were operating in other parts of them (e.g., Figs 5, 8). This can be explained by a high gas saturation in the roof of the aquifer, and the formation of a front of pore fluids, migrating outward from the center of the contact (interface) zone, between the aquifer and the caprock. As a result of the phenomena described from the contact zone, the process of CO_2 desequestration, associated with the dissolution of carbonate minerals, was operating in the lower part of caprock (Fig. 9).

CONCLUSIONS

When modelling the impact of CO_2 storage on the aquifer and caprock contact zone, it was noted that small decreases in porosity, resulting from a positive balance of the secondary minerals volume, were visible mainly in the aquifer rocks. Porosity remained almost constant in the caprock, which is advantageous for the sealing properties of the repository.

It also was observed that the mineralogical changes, visible in the contact zone, were different from those that occurred in the remaining parts. This can be explained by the high gas saturation in the aquifer roof, on the other hand, by the formation of a front of pore fluids migrating outwards from the center of the contact zone of both rock types. These mechanisms caused the temporary release of CO_2 at the base of the insulating layer, associated with the dissolution of carbonate minerals.

The practical application for the results of this study are assessment of the amounts of carbon dioxide, trapped by dissolution and in mineral phases, and also evaluation of the petro-structural consequences of CO_2 injection into saline aquifers of the Upper Silesian Coal Basin. This allows the estimation of the suitability of the formations for CO_2 storage.

Acknowledgments

Alla Shogenova (Tallinn University of Technology) and Adam Wójcicki from (Polish Geological Institute) are acknowledged for their comments, which contributed to improvements to of the article.

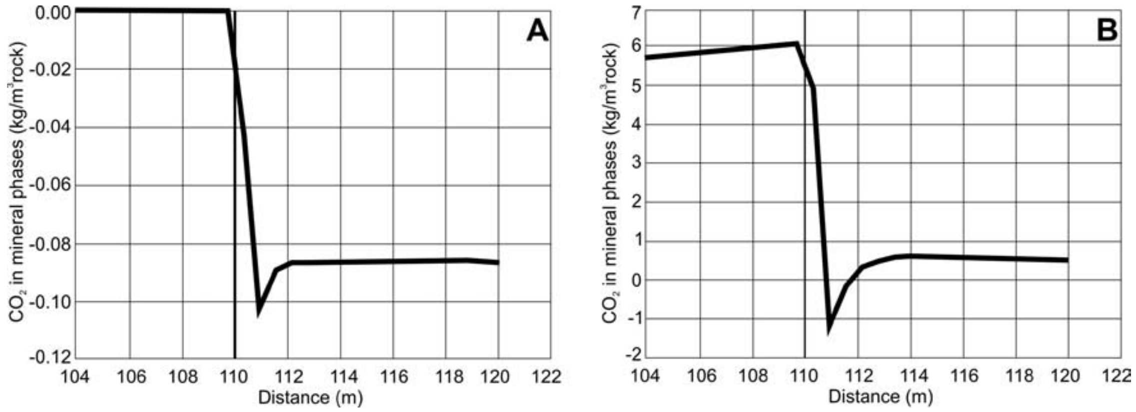

Fig. 9. Amounts of CO_2 trapped in mineral phases (kg/m^3 rock) in vertical distance from injection point after: **A** – 1 year and **B** – 20,000 years of storage (explanations as in Fig. 2)

This work was supported by Polish Ministry of Science and Higher Education (grant N N525 363137).

REFERENCES

Bethke, C. M., 2008. *Geochemical and Biogeochemical Reaction Modeling*. Cambridge University Press, Cambridge, 543 pp.

Bildstein, O., Kervéva, C., Lagnea, V., Delaplac, P., Crédo, A., Audigan, P., Perfetti, E., Jacquemet, N. & Jullien, M., 2010. Integrative modeling of caprock integrity in the context of CO_2 storage: evolution of transport and geochemical properties and impact on performance and safety assessment. *Oil & Gas Science and Technology – Revue de IFP*, 65: 485–502.

Corey, A. T., 1954. The interrelations between gas and oil relative permeabilities. *Producers Monthly*, 19: 38–41.

Credoz, A., Bildstein, O., Jullien, M., Raynal, J., Pétronin, J. C., Lillo, M., Pozo, C. & Geniaut, G., 2009. Experimental and modeling study of geochemical reactivity between clayey caprocks and CO_2 in geological storage conditions. *Energy Procedia*, 1: 3445–3452.

Gaus, I., Azaroual, M. & Czernichowski-Lauriol, I., 2005. Reactive transport modelling of the impact of CO_2 injection on the clayey cap rock at Sleipner (North Sea). *Chemical Geology*, 217: 319–337.

Johnson, J. W., Nitao, J. J. & Knauss, K. G., 2004. Reactive transport modeling of CO_2 storage in saline aquifers to elucidate fundamental processes, trapping mechanisms, and sequestration partitioning. In: Baines, S. J. & Worden, R. H. (eds), *Geologic Storage of Carbon Dioxide*. *Geological Society, Special Publication*, 233: 107–128.

Karwasiecka, M., 2001. The geothermal field of the Upper Silesian Coal Basin. *Technika Poszukiwań Geologicznych, Geosynoptyka i Geotermia.* 40: 41–49. [In Polish, English Summary].

Kaszuba, J. P., Janecky, D. R. & Snow, M. G., 2005. Experimental evaluation of mixed fluid reactions between supercritical carbon dioxide and NaCl brine: relevance to the integrity of a geologic carbon repository. *Chemical Geology*, 217: 277–293.

Labus, K., 2005. Origin of groundwater mineralization in coarse-grained Lower Badenian aquifer in the Czech part of the Upper Silesian Coal Basin. *Geological Quarterly*, 49: 75–82.

Labus, K., 2007. Identification of the processes controlling the groundwater chemical composition under mine drainage conditions within the south-western part of the Upper Silesian Coal Basin. *Zeszyty Naukowe Politechniki Śląskiej*, 1769: 1–247. [In Polish, English summary].

Labus, K. & Bujok, P., 2011. CO_2 mineral sequestration mechanisms and capacity of saline aquifers of the Upper Silesian Coal Basin (Central Europe) – Modeling and experimental verification. *Energy*, 36: 4974–4982.

Labus, K., Tarkowski, R. & Wdowin, M., 2010. Assessment of CO_2 sequestration capacity based on hydrogeochemical model of water-rock-gas interactions in the potential storage site within the Bełchatów area (Poland). *Mineral Resources Management*, 36: 69–84.

Liu, F., Lu, P., Griffith, C., Hedges, S. W., Soong, Y., Hellevang, H. & Zhu, C., 2012. CO_2–brine–caprock interaction: Reactivity experiments on Eau Claire shale and a review of relevant literature. *International Journal of Greeonhouse Gas Control*, 7: 153–167.

Navarre-Sitchler, A., Muouzakis, K., Heath, J., Dewers, T., Rother, G., Wang, X, Kaszuba, J. & McCray, J., 2011. Changes to porosity and pore structure of mudstones resulting from reaction with CO_2 and brine. *Mineralogical Magazine*, 75: 1527.

Palandri, J. L. & Kharaka, Y. K., 2004. A compilation of rate parameters of water-mineral interaction kinetics for application to geochemical modeling. *US Geological Survey. Open File Report*, 2004-1068: 1–64.

Pruess, K., 2004. The TOUGH Codes – A family of simulation tools for multiphase flow and transport processes in permeable media. *Vadose Zone Journal,* 3: 738–746.

Spycher, N. & Pruess, K., 2005. CO_2-H_2O mixtures in the geological sequestration of CO_2: II. Partitioning in chloride brines at 12–100°C and up to 600 bar. *Geochimica et Cosmochimica Acta*, 69: 3309–3320.

Steefel, C. I., 2001. *Crunch*. Lawrence Livermore National Laboratory, Livermore, California, 76 pp.

van Genuchten, M. T., 1980. A closed-form equation for predicting the hydraulic conductivity of unsaturated soils. *Soil Science Society of America Journal*, 44: 892–898.

Xiao, Y., Xu, T. & Pruess, K., 2009. The effects of gas–fluid-rock interactions on CO_2 injection and storage: insights from reactive transport modeling. *Energy Procedia*, 1: 1783–1790.

Xu, T., Apps, J. A. & Pruess, K., 2005. Mineral sequestration of carbon dioxide in a sandstone–shale system. *Chemical Geology*, 217: 295–318.

Xu, T., Apps J. A. Pruess, K. & Yamamoto, H., 2007. Numerical modeling of injection and mineral trapping of CO_2 with H_2S and SO_2 in a sandstone formation. *Chemical Geology*, 242: 319–346.

Xu, T., Sonnenthal, E. L., Spycher, N. & Pruess, K., 2006. TOURGHREACT: A simulation program for non-isothermal multiphase reactive geochemical transport in variably saturated geologic media. *Computer & Geosciences*, 32: 145–165.